Standard and viscoelastic mechanical properties of respiratory system compartments in dogs: effect of volume, posture, and shape.

D'Angelo Edgardo[a]*, Calderini Edoardo[c], Tavola Mario[b], and Pecchiari Matteo[a]

[a] Department of Physiopathology and Transplantations, Università degli Studi di Milano, Milan, Italy.

[b] Division of Anesthesia and Intensive Care, Fondazione IRCSS Cà Granda, Ospedale Maggiore Policlinico, Milan, Italy.

[c]Division of Anesthesia and Intensive Care, Ospedale di Lecco, Lecco, Italy.

DOI: http://dx.doi.org/10.1016/j.resp.2018.12.003

*Corresponding author: Edgardo d'Angelo, Università degli Studi di Milano, Dipartimento di Fisiopatologia e dei Trapianti, via Mangiagalli 32, 20133 Milan, Italy

E-mail address: edgardo.dangelo@unimi.it

ABSTRACT

In 9 anesthetized, paralyzed dogs lung and chest-wall standard (viscous resistance, Rint, and quasi-static elastance, Est) and viscoelastic parameters (resistance, Rvel, and time constant, τvel) were measured in the supine posture before and after rib-cage block, after application of an expiratory threshold load, and after 75° head-up tilting before and after wide chest opening. Lung and chest-wall τvel were the same under all conditions. Rvel was independent of volume and posture, and greater for the lung. Chest-wall Rint was independent of flow, volume, and posture. Lung Rint decreased with increasing volume. Chest-wall Rint, Est and Rvel increased with rib-cage block, allowing the assessment of both abdominal-wall and rib-cage characteristics. When chest opening did not elicit bronchoconstriction, the decrease of Rvel was ~6%. Main conclusions: lung and chest-wall exhibit linear tissue viscoelasticity within the range studied; rib-cage and abdomen characteristics are similar, and asynchronous motion is not expected at physiological respiratory rates; in normal lungs, heterogeneity of parallel time constants plays a marginal role.

Keywords

Abdominal wall, airway resistance, chest wall, lung, mechanics, rib cage, viscoelasticity

1. Introduction

In 1955, Mount (1955) proposed a viscoelastic model of the lung which could account for the inverse frequency dependence of both dynamic work and compliance observed in open-chest rats. This model was subsequently used to explain lung and chest wall stress relaxation data obtained in anesthetized, paralyzed normal subjects (Sharp et al., 1967). When both airway opening and esophageal pressure are measured, the technique of the end-inflation, rapid airway occlusion during constant flow ($\dot{V}$) inflation of the relaxed respiratory system allows the assessment of the resistance due to air flowing along the airways and velocity of tissue strain (Rint), the lung and chest wall quasi-static elastance (Est), herein defined as standard characteristics, and the additional resistance (ΔR) which mainly results from viscoelatic pressure dissipation within the lung and chest wall tissues (Bates et al., 1988a).

The results obtained with this procedure in healthy humans (D'Angelo et al., 1989; 1991; 2000) and normal animals (Bates et al., JAP 1989a; Similowski et al., 1989; Shardonofsky et al., 1991; D'Angelo et al., 2002; 2008) have shown the relevant role played by viscoelastic properties in the dynamic response of the respiratory system and its components. Viscoelastic elements, acting as shock absorber, represent an effective protection of tissues against abnormal stresses that occur at high rates mainly in the lungs, especially diseased lungs. Furthermore, viscoelastic properties have important implications in terms of respiratory work (D'Angelo et al., 1989; 1999), passive lung deflation (Bates et al., 1985; Chelucci et al., 1991), performance of forced expiratory vital capacity maneuvers especially in obstructed patients (D'Angelo et al., 1993; 1994a: ATS/ERS 2005), and frequency dependence of elastance and resistance (Hantos et al., 1986).

All these studies have been performed in the supine posture at the relatively low end-expiratory lung volumes typical of paralysis, and with ventilatory patterns resembling normal quite breathing. Furthermore, no attempt has been ever made to partition the standard and the viscoelastic characteristics of the chest wall between rib cage and abdominal wall, nor to examine the dependency of lung and chest wall viscoelastic properties on posture, shape, and volume. These issues have been therefore examined in anesthetized, paralyzed, artificially ventilated dogs using the technique of the end-inflation, rapid airway occlusion during constant flow inflation.

In the lung, stress relaxation can also originate from the non uniform distribution of parallel (standard) time constants (Rint/Est), due to airway resistance and tissue compliance heterogeneities. Indeed, the same equations describe the mechanical response to constant flow inflations and sustained post-inflation airway occlusion in the presence of viscoelastic elements or inequalities of standard time constants (Lorino et al., 1994). Hence, an attempt has been made to assess the impact of the non uniform distribution of standard time constants by comparing the post-inflation decay of

transpulmonary pressure occurring before and after wide opening of the thorax. These measures have been performed in the head-up posture, in which the top-to-bottom difference of pleural surface pressure and the dependent heterogeneity of standard time constants are the largest in the intact, normal dog (D'Angelo et al., 1970).

2. Methods

Nine, adult mongrel dogs (weight range 14-23 kg) were anesthetized with pentobarbital sodium (20 $mg \cdot kg^{-1}$), after induction with diazepam (10 $mg \cdot kg^{-1}$). Absence of withdrawal and corneal reflexes was used to assess the adequacy of anesthesia. The animals were placed supine on a tilting table; with head and hips secured to the table, they could be tilted 75° head-up. Rectal temperature was maintained at 37-38°C by means of a heated blanket. In open-chest animals, lungs and heart were repeatedly wetted with warmed saline, temperature being kept by a lamp.

A metal cannula, connected to a pneumotachograph, and two polyethylene catheters were inserted into the trachea, jugular vein, and carotid artery, respectively. A thin walled latex balloon (6 cm long, 4 cm circumference), sealed over a polyethylene catheter (1.8 mm ID) with multiple holes over the balloon length, and filled with 0.8-1 ml of air, was placed in the esophagus. Airflow ($\dot{V}$) was measured with a heated Fleisch pneumotachograph no.1 (HS Electronics, March-Hugstetten, Germany) connected to the tracheal cannula and a differential pressure transducer (Validyne MP45, ±2 cmH_2O; Northridge, CA). The response of the pneumotachograph was linear over the experimental flow range. Tracheal (Pao), esophageal (Pes), and systemic blood pressure were measured with pressure transducers (8507C-2 Endevco, San Juan Capistrano, CA; Statham P23Gb, HS Electronics, March-Hugstetten, Germany) connected to the side arm of the tracheal cannula, the esophageal and carotid catheter, respectively. The signals from the transducers were amplified (RS3800; Gould Electronics, Valley View, OH) and recorded on tape (Racal Store 7DS, Southampton, England). No appreciable shift or amplitude change occurred in the signals up to 20 Hz.

After completion of the procedures above, the dogs were paralyzed with pancuronium bromide (0.1 $mg \cdot kg^{-1}$); anesthesia and complete muscle relaxation were maintained by continuous infusion of pentobarbital sodium (4 $mg \cdot kg^{-1} \cdot h^{-1}$) and pancuronium bromide (0.05 $mg \cdot kg^{-1} \cdot h^{-1}$). Adequacy of anesthesia was ensured by the absence of sudden increases in heart rate and/or systemic blood pressure. The occlusion method (Baydur et al., 1982), adapted for the state of paralysis, was used to check the correct position of the esophageal balloon in the supine and head-up posture. Arterial blood P_{O_2}, P_{CO_2} and pH were measured by means of a blood gas analyzer (IL 1620; Instrumentation Laboratory, Milan, Italy) on samples drawn every 9-10 minutes. They

remained essentially constant throughout the experiments averaging 90±6 and 38±3 mmHg, and 7.36±0.04, respectively.

The animals were mechanically ventilated with a Servo ventilator (900C; Siemens, Berlin, Germany), the inspiratory and expiratory port being connected via an Y piece to the pneumotachograph by means of very low-compliance tubing (20 cm long, 2 cm ID). A normally open, fast solenoid valve (closing time 5-8 ms, depending on pressure in the line), placed between the Y connector and the pneumotachograph, could be activated via the ventilator to produce an end-inflation pause of 5 s. The added dead space was 10 ml. In addition, a three way stopcock allowed the connection of the expiratory port of the ventilator either to the ambient or to a drum in which the pressure could be adjusted by means of a flow-through system. End-expiratory occlusions lasting 2-3 s were repeatedly performed: absence of a concomitant increase of Pao ensured the absence of intrinsic end-expiratory positive pressure. To assess the postural difference in the end-expiratory lung volume (EELV), as well as the pressure to be applied in the supine posture to reproduce the head-up EELV, the dog was tilted head-up, the ventilator was stopped with the valves closed, the dog was brought back to the supine posture, Pao was noted, and the expiratory valve was opened to measure the expired volume.

2.1. Procedure and data analysis

The baseline ventilator settings (on SIMV mode) were a fixed tidal volume (V_T) of 9-12 $ml \cdot kg^{-1}$, an inspiratory duration (T_I) of 1.5 s, and a frequency of 12-15 min^{-1}, adjusted to keep normocapnia (Pa_{CO_2}=37±3 mmHg) and normoxia (Pa_{O_2}=90±7 mmHg) throughout the experiment. Test breaths were characterized by the introduction of a 5 s end-inflation pause. Two types of test breaths were used: 1) while keeping V_T constant (0.24±0.04 l), $\dot{V}$ was changed in the range 0.06–1.20 $l \cdot s^{-1}$ by adjusting T_I for single breaths with the corresponding dial of the ventilator, and 2) while keeping $\dot{V}$ constant (0.19±0.06 $l \cdot s^{-1}$), V_T was changed in the range 0.07–0.72 l by adjusting the frequency dial of the ventilator for single breaths. The latter tests were performed only in the supine posture with normal EELV. Each type of test breath was applied three times, while 3-4 baseline inflations were inserted between test breaths. Before each group of tests, the respiratory system was inflated 2-3 times to 25-30 cmH_2O to ensure a fixed volume history.

In the supine posture, the animals were studied under the following conditions: a) unrestrained chest wall expansion; b) block of rib cage expansion; and c) application of an expiratory threshold load. Rib cage block was obtained by means of casts made of plaster of Paris, allowing the anterior abdominal wall between the costal arches to move freely. EELV reduction was monitored by Pes and volume changes on cast application and removal. The expiratory

threshold load (ETL) was applied by connecting the expiratory port to the drum, where pressure was adjusted in order to reproduce the EELV of the head-up posture. In the head-up posture, the animals were studied both with closed and open chest. To prevent EELV changes on chest opening, the ventilator was stopped with the valves closed, the chest was widely opened, the pressure in the drum was set equal to the concomitant Pao, the expiratory port was connected to the drum, and ventilation was resumed. The sternum was removed, and the ribs and diaphragm were pulled widely apart in order to prevent appreciable contacts with the lung. Fig. 1 shows schematically the temporal sequence of the conditions studied, the interventions performed, and the concomitant changes in Pao, EELV and end-expiratory Pes. Thereafter, the animals were killed with an overdose of anesthetics. In four animals, however, baseline ventilation at preserved EELV was continued for ~10 min after heart arrest, and test breaths (fixed V_T, various $\dot{V}$) with an increased duration (20 s) of the end-inflation occlusion were applied.

From tape playback without filtering and at the same speed as during recording, signals were digitized at a sampling rate of 200 Hz with a 14-bit A/D converter and displayed on the screen of a waveform analayzer (Data 6000, Analogic Co., Peabody, MA) connected to a desk computer (Hewlett-Packard 300/9000). Volume changes (ΔV) were obtained by numerical integration of the digitized airflow signal. Data were interpreted according to a viscoelastic model of the respiratory system, in which each component was made by a Kelvin body with a dashpot in parallel (Bates et al., 1985; D'Angelo et al, 1991). The end-inflation occlusions were followed by a rapid initial drop of Pao, and Pes ($P_{1,RS}$, and $P_{1,W}$), and a slow decay ($P_{2,RS}$ and $P_{2,W}$) to plateau values, taken to represent the quasi-static elastic recoil pressure of the respiratory system ($Pst_{,RS}$) and chest wall ($Pst_{,W}$), respectively. Respiratory system and chest wall interrupter ($Rint_{,RS}$ and $Rint_{,W}$) and additional resistance ($\Delta R_{,RS}$ and $\Delta R_{,W}$) were obtained dividing the corresponding P_1 and P_2 by the flow preceding the occlusion. Viscoelastic parameters were computed from the values of $\Delta R_{,RS}$ or $\Delta R_{,W}$ measured at different T_I using the function

$$\Delta R = Rvel \cdot (1 - e^{-T_I/\tau_{vel}}) \quad (1)$$

where Rvel and τvel are viscoelastic resistance and time constant, respectively. Finally, respiratory system ($Est_{,RS}$) and chest wall quasi-static elastance ($Est_{,W}$) equalled $Pst_{,RS}$ and $Pst_{,W}$ divided by V_T. Lung parameters ($Rint_{,L}$, $\Delta R_{,L}$ and $Est_{,L}$) were computed as differences between the corresponding parameters pertaining to the respiratory system and chest wall, while $\Delta R_{,L}$ values were used in *Eq.1* to obtain $Rvel_{,L}$ and $\tau vel_{,L}$.

All procedures were performed in accordance with the National Institutes of Health guide for animal care (NIH publications No. 8023, revised 1978) and the rules in force at the time in Italy.

2.2. Statistics

Analyses were performed using SPSS 11.5 (SPSS Inc., Chicago, IL). Data are presented as mean±SD, unless stated otherwise. Comparisons among conditions were performed using repeated measuremebts ANOVA, followed by post-hoc (t-test, with Bonferroni correction) when needed. Regression analysis was performed using the least square method. The level for statistical significance was taken at $p \leq 0.05$.

3. Results

The mean values of the mechanical variables assessed during fixed V_T inflations are reported in Table 1. Variables measured in the supine posture during normal expansion of the relaxed respiratory system at the beginning of the experimental sequence and just before head-up tilting did not differ significantly; the corresponding values were therefore averaged. Rint was constant over the experimental flow range both for the chest wall and lung (Fig. 2), and larger for the latter than the former ($\Delta Rint=0.24\pm0.25$ $cmH_2O \cdot s \cdot l^{-1}$; $p=0.024$). Est was also independent of flow, and markedly larger for the lung than the chest wall ($\Delta Est=15.7\pm6.9$ $cmH_2O \cdot l^{-1}$; $p<0.001$). $Est_{,RS}$ and $Est_{,L}$ were linearly related (1.03 ± 0.08; $p<0.001$), whilst $Est_{,RS}$ and $Est_{,W}$ were unrelated (-0.03 ± 0.08; $p=0.744$); part of $Est_{,RS}$ variability could be accounted for by the animal size ($r=0.770$; $p=0.015$). No relation was found between $Rint_{,W}$, and $Rint_{,L}$ (0.25 ± 0.39; $p=0.540$).

ΔR decreased with increasing flow at constant V_T, and therefore increased with increasing T_I (Fig. 3). ΔR-T_I data fitted *Eq.1* accurately ($r \geq 0.932$), thus allowing the computation of Rvel and τvel. This was true for the respiratory system, chest wall, and lung. Like Rint, Rvel was independent of flow, and larger for the lung than for the chest wall ($\Delta Rvel=4.1\pm2.9$ $cmH_2O \cdot s \cdot l^{-1}$; $p=0.002$). In contrast, τvel was the same for all compartments, averaging 1.18 ± 0.15 s (range 0.87-1.57 s).

3.1. Effect of rib cage block

Table 1 shows the mean values of the mechanical variables obtained during fixed V_T inflations of the respiratory system with impeded expansion of the rib cage. As with unrestrained expansion, Rint and Est were independent of flow, while ΔR still depended on T_I alone. Rib cage block caused a marked increase of $Rint_{,RS}$, $Est_{,RS}$, and $Rvel_{,RS}$, whereas τvel was unaffected and the same for all compartments, (1.19 ± 0.13 s; range: 0.94-1.49 s). The increase of $Rint_{,RS}$ and $Est_{,RS}$ was contributed mainly by the chest wall (80 %), whereas the changes of $Rvel_{,RS}$ were essentially due to those of $Rvel_{,W}$ (Table 1 and Figure 4). No relationship was found between the changes of $Rvel_{,W}$ and $Rint_{,W}$ ($r=0.396$; $p=0.457$) or $Est_{,W}$ ($r=0.292$; $p=0.216$).

3.2. Effect of volume, posture, and shape

The effect of volume was studied by means of 1) inflations of different V_T and fixed $\dot{V}$ starting from the normal, supine EELV; and 2) inflations of different $\dot{V}$ and fixed V_T taken from an elevated EELV in the supine and head-up posture (Fig. 1). ETL increased EELV in the supine posture by essentially the same amount as did tilting. However, the rib cage transverse diameter, measured with an anatomical caliper at the level of the 4^{th} to 6^{th} rib, decreased by ~14% with tilting, but increased by ~8% with ETL. These measures clearly indicate a substantially different chest wall shape at iso-lung volume between the supine and head–up posture, in line with previous observations (D'Angelo et al., 1973).

With constant $\dot{V}$ inflations from normal supine EELV, $R_{int,RS}$ and $R_{int,L}$ decreased curvilinearly with increasing V_T, whereas $R_{int,W}$ did not vary; thus, lung conductance ($G_{int,L}$) increased linearly with volume (Fig. 2), the slope (range 0.11–0.67 $l \cdot s^{-1} \cdot cmH_2O^{-1}$) of this relation being significant in all dogs. With constant V_T inflations in the head-up posture or from elevated EELV in the supine posture, Rint was still independent of flow. With respect to values obtained with constant V_T inflations from the normal supine EELV, $R_{int,L}$ decreased, while $R_{int,W}$ remained unchanged (Table 1). Indeed, data of $R_{int,L}$ and $R_{int,W}$ of normal head-up and supine dogs with ETL fell along the corresponding Rint–V relationship obtained with inflations initiated from normal supine EELV (Fig. 2).

Fig. 4 shows the relations between the changes of quasi-static transpulmonary (ΔP_L) or chest wall pressure (ΔP_W) and volume above supine EELV (ΔV) obtained in the head-up and supine posture under various conditions. While the ΔP_W–ΔV relationship was linear under all conditions, that between ΔP_L and ΔV was sigmoidal; however, the quasi-static elastance was essentially the same (26.8±6.1 $cmH_2O \cdot l^{-1}$) in the volume range 0.07-0.43 l. ΔP_L-ΔV data of head-up dogs fell along the relation of supine animals; in fact, $E_{st,L}$ was not significantly different from that observed in the supine dogs with ETL (Table 1). In contrast, ΔP_W-ΔV data were displaced markedly to the left of the supine ΔP_W–ΔV relationship; at the same volumes, $E_{st,W}$ was in fact 1.5 times that observed in the supine posture (Fig. 4 and Table 1).

No significant modification of the viscoelastic parameters occurred in the supine posture by changing the inflation volume at fixed flow or the inflation flow at fixed V_T both in dogs with normal and elevated EELV, or by moving from the supine to the head-up posture (Fig. 5 and Table 1).

3.3. Effect of chest wall removal

The effects of opening the chest are summarized in Table 2: $Rint,_L$ doubled, while $Est,_L$, $Rvel,_L$, and $\tau vel,_L$ were unchanged. However, the increase of $Rint,_L$ was significant in 5 dogs ($\Delta Rint,_L$=1.4±0.3 $cmH_2O \cdot s \cdot L^{-1}$; $p<0.001$), but not in the other 4 animals ($\Delta Rint,_L$=0.0±0.2 $cmH_2O \cdot s \cdot L^{-1}$; p=0.925), whereas in the same 5 and 4 dogs, $Rvel,_L$, increased ($\Delta Rvel,_L$=2.2±1.0 $cmH_2O \cdot s \cdot L^{-1}$; p=0.008) and decreased significantly ($\Delta Rvel,_L$=-0.5±0.2 $cmH_2O \cdot s \cdot L^{-1}$; p=0.019), respectively (Figure 6). No relation occurred between $Rint,_L$ or $Rvel,_L$ before chest opening and $\Delta Rint,_L$ (r=0.244; p=0.526) or $\Delta Rvel,_L$ (r=0.171; p=0.661).

3.4. Time dependency of viscoelastic parameter evaluation

Table 3 shows values of $Rvel,_L$, and $\tau vel,_L$ computed in four isolated lungs before and after heart arrest from measurements of $P_{2,L}$ made at 5 and 20 s from the end-inflation occlusion of test breaths with fixed V_T and various $\dot{V}$. There was no significant difference between parameters computed from measures made at 5 s from airway occlusion before and after heart arrest, i.e in the presence and absence of gas exchange. Similarly, there was no significant difference between parameters computed from measures made after heart arrest at 5 and 20 s from occlusion, indicating that *Eq.1* can be appropriately used to assess tissue viscoelastic properties.

4. Discussion

The present results have shown that under all the conditions studied the mechanical behavior of the respiratory system is accurately reproduced by a model in which each component of the respiratory system, lung, chest wall, rib cage and abdominal wall, is made of a Kelvin body with a dashpot in parallel, as indicated by the electrical analogue shown in Fig. 7. For the first time, the standard (Rint and Est) and viscoelastic properties (Rvel and τvel) of the chest wall in the supine dog have been directly partitioned into those of the rib cage and abdominal wall, while the assessment of lung and chest wall mechanical properties has been extended to a wider range of volumes and flows. Also for the first time, the viscoelastic properties have been studied in the head-up posture, together with the standard characteristics, both before and after wide opening of the thorax, thus allowing the assessment of the contribution of heterogeneity of parallel time constant. The results have shown that in relaxed dogs, lung and chest wall tissues behave as a linear mechanical system in the mid-lung volume range.

Standard and viscoelastic parameters of lung and chest wall have been previously assessed with the present procedure in 6 anesthetized, paralyzed dogs, though limitedly to unrestrained expansion of the respiratory system from normal EELV in the supine posture (Similowski et al.,

1989); under this condition, the mean values of the parameters obtained herein (Table 1) do not differ significantly ($P \geq 0.256$) from those reported in that study.

4.1. Modeling the respiratory system

The slow decay of Pao and Pes to an apparent stable value after the rapid end-inflation airway occlusion ($P_{2,RS}$ and $P_{2,W}$) has been entirely attributed to the viscoelastic behavior (stress relaxation) of lung parenchyma and chest wall tissues, respectively (Fig. 7). Heterogeneity of airway resistance and parenchymal compliance, leading to differences in regional standard time constants (Rint/Est) and dependent pendelluft, can in fact contribute to $P_{2,L}$, and hence $P_{2,RS}$, with a consequent increase of $Rvel_{,L}$ and $Rvel_{,RS}$. The suppression of most if not all of these heterogeneities with the exposure of the lung to the ambient has shown that the contribution is marginal: in the group of animal in which $Rvel_{,L}$ decreased with this intervention (Group#1 in Fig. 6), the fall averaged only 6% of pre-intervention values. This observation also indicates that local differences of alveolar pressure during passive lung inflations should be minor even in the head-up intact dog, when the gravity dependent heterogeneity of lung standard time constants should be maximal (D'Angelo et al., 1970). Indeed, only very small differences among directly measured local alveolar pressure were found in supine, intact dogs (Bates et al., 1988b; 1989b), although it should be noted that the gravity dependent heterogeneity of regional lung expansion, and hence lung standard time constants, is expected to be less pronounced in this posture (D'Angelo et al., 1970).

Assessment of P_2 in living animals can be undesirably affected by continuing gas exchange during the maintained post-inflation occlusion (Hughes et al., 1959). Furthermore, on the basis of stress relaxation data obtained in excised cat lungs (Hildebrandt, JAP 1969), it has been suggested that the evaluation of viscoelastic time constant might be heavily dependent on the time from the end-inflation occlusion at which P_2, and hence ΔR, are measured (Wilson, 1994). However, the data reported in Table 3 show that within the reported limits, neither gas exchange nor the timing of P_2 measure affect the assessment of both $Rvel_{,L}$ and τvel appreciably.

The present model does not take into account inertia and dry friction. With the present modality of inflation, appreciable accelerations occurred only at the time of the end-inflation occlusion, making the introduction of inductance in the model unnecessary. To justify energy dissipation during sinusoidal oscillations of isolated cat lungs, Hildebrandt (1970) has introduced Prandtl in addition to Maxwell bodies, and the same has been done by Stamenovic et al. (1990) to explain certain aspects of the mechanical behavior of the chest wall in humans. While Prandtl bodies might have contributed to Pst, they could not have affected P_2, as flow was not inverted at this point in time.

In Mount's model, a single Maxwell body (capacitance and a resistor in parallel in Fig. 7) confers viscolelastic behavior to lung and chest wall tissues. In contrast, on the basis of stress relaxation data obtained in isolated cat lungs, Hildebrandt (1970), proposed a model in which the viscoelastic compartment is made by linear material with a continuous distribution of time constants, the mechanical analogue being represented by a number of Maxwell bodies arranged in parallel (Stamenovich et al., 1990). Although the Mount's model has the advantage of allowing the identification of the physiological counterparts of estimated parameters, it likely represents an oversimplification. Indeed, an analysis of lung impedance data obtained in dogs between 0.1-5 Hz has led to the conclusion that the Hildebrandt's model is superior to Mount's model in fitting performance, although this superiority seems limited to the lowest frequencies (Hantos et al., 1990). On the other hand, other impedance data obtained in dogs and humans (Ingram and Pedley, 1986; Bates et al., 1989b) could be adequately fitted with the Mount's model also at frequencies ≤0.1 Hz (D'Angelo et al., 2000), favoring the conclusion that analyses based on either model give comparable estimates of effective (viscous plus viscoelastic) resistance of normal lungs (Harf et al., 1990; Bates et al., 1986).

4.2. Partitioning of chest wall characteristics

Lung volume changes occur because of the displacement of the pulmonary part of the rib cage (i.e. that facing the lung) and of the diaphragm, which in turn results in the displacement of the antero-lateral abdominal wall and the abdominal part of the rib cage (i.e.. that facing the abdominal contents) (D'Angelo and Agostoni, 1995). The pulmonary part of the rib cage and the antero-lateral abdominal wall together with the abdominal part of the rib cage, hereafter indicated as the rib cage and the abdominal wall, respectively, may be considered to operate in parallel (Fig. 7). Indeed, 1) the mechanical linkage between the rib cage and the abdominal wall in humans and dogs (Estenne et al., 1985; Deschamps et al., 1987; D'Angelo et al., 1973), or between the pulmonary and abdominal part of the rib cage in rabbits and dogs (D'Angelo et al., 1973; D'Angelo and Sant'Ambrogio, 1974; Jiang et al., 1987) is trivial or absent; and 2) during passive expansion of the relaxed respiratory system there is a unique relationship between pleural and abdominal pressure changes, whereby standard and viscoelastic properties can be profitably assessed using pleural pressure. In the attempt to block only the lung apposed part of the rib cage, thus allowing the assessment of the mechanical properties of the abdominal wall, the cast was made to reach the 8^{th} rib ventrally and 9^{h} rib dorsally. In line with previous studies (D'Angelo et al., 1973; Agostoni et al., 1988), direct observations in the present supine dogs indicate in fact that the lung border does not reach the 9^{th} intercostal space dorsally, even with the largest V_T.

Apart from the modest but significant increase of Est,L, likely the consequence of distortion, the changes of respiratory system parameters with rib cage block reflect those of the chest wall (Table 1), which should in turn correspond to those of the abdominal wall. The rib cage parameters can be then computed from the latter and those of the chest wall obtained during unrestrained expansion of the respiratory system. Accordingly, for the rib cage the mean values of Rint, Est, Rvel should be 2.0±1.1 $cmH_2O \cdot s \cdot l^{-1}$, 19.9±3.2 $cmH_2O \cdot l^{-1}$, and 9.7±5.3 $cmH_2O \cdot s \cdot l^{-1}$, respectively, τvel being necessarily equal to that of the abdominal wall because the latter was in turn equal to that of entire chest wall (Table 1). Although somewhat lower for the rib cage, Rint (p=0.665), Est (p=0.517), and Rvel (p=0.830) did not differ significantly from those of the abdominal wall (Table 1), the same applying to the standard time constant (Rint/Est; 0.09±0.04 vs 0.10±0.04 s; p=0.751). Rib cage and abdominal wall mechanical properties are therefore similar. Even taking the difference in the standard time constant as true, an appreciable increase (≥1%) in the ratio rib cage to abdominal volume change would occur with sinusoidal cycling at frequencies >1 Hz.

Current views concerning chest wall partitioning (D'Angelo and Agostoni, 1995), adopted herein, imply that the extension of the (pulmonary) rib cage and the abdominal wall changes with the lung volume, thus causing substantial problems for the measure of the volume contributions of these compartments and the computation of their compliance. This, however, does not seem to be the case in the supine dog, because abdominal and chest wall compliance, and hence that of the rib cage, were independent of lung volume changes at least up to 0.4 l from EELV (Fig. 4).

4.3. Viscous and viscoelastic resistance

Rint ($P_1/\dot{V}$) represents the viscous resistance, because P_1 occurs simultaneously with airflow interruption. Rint,W was independent of flow, volume, and posture (Fig. 2 and Table 1); it likely represents an intrinsic property of chest wall tissues, in spite of their apparent heterogeneities and differences in the pattern of motion under the various experimental conditions. Like Rint,W, Rint,L was independent of posture and flow, at least up to 0.05 $l \cdot s^{-1} \cdot kg^{-1}$, but decreased with increasing the lung volume (Fig. 2 and Table 1). While Rint,W reflects the viscous resistance of chest wall tissues only, Rint,L is the sum of airway (Raw) and lung tissue resistance. It has been shown, however, that Rint,L reflects Raw, with little or no contribution from lung tissue (Bates et al., 1988b;1989b). This is supported by the present observation that Rint,L decreased significantly with increasing lung volume independent of how the increase was obtained: V_T augmentation from normal EELV, or elevation of EELV in the supine posture, or shift from the supine to the head-up posture (Fig. 2 and Table 1). Further support is provided by the linear, positive relationship between Gint,L and lung volume (Fig. 2); similar relationships have been in fact demonstrated in anesthetized, paralyzed

humans using the present method (D'Angelo et al., 2000), and between lung volume and airway conductance directly in spontaneously breathing subjects using the plethysmographic technique (Briscoe and Bubois, 1958). It should, however, be noted that the difference between $R_{int,W}$ and $R_{int,L}$ became substantial only at low volumes (Fig. 2), suggesting that the volume dependence of $R_{int,L}$ might play a marginal role during normal or moderately enhanced breathing.

Viscolelastic parameters, Rvel, τvel, and hence Evel, were independent of volume, flow, and posture; this was the case for both the lung and chest wall (Table 1). In the volume range of the present experiment, the results are thus consistent with linear viscoelasticity of respiratory system tissues. A similar conclusion was reached for tissue viscoelasticity of isolated dog lungs investigated by means of small-amplitude volume oscillations (Hantos et al., 1990).

While the difference between $R_{int,L}$ and $R_{int,W}$ was small or inconsistent, that between lung and chest wall Rvel was marked (Table 1 and Fig. 3); energy dissipation during tidal breathing should be therefore substantially larger for the lung than chest wall. Using the parameters reported in Table 1 for unrestrained chest expansion, during sinusoidal oscillations of fixed amplitude, the ratio of lung to chest wall energy dissipation (R_{ED}) decreases with frequency (f). In the range 0.1-4 Hz, a good fit ($r^2 \geq 0.999$) is provided by the function $R_{ED}=1.23+0.67 \cdot e^{-2.85 \cdot f}$ and $R_{ED}=1.01+0.69 \cdot e^{-2.61 \cdot f}$ in the supine and head-up posture, respectively. At variance with anesthetized, paralyzed dogs, the difference between $R_{int,L}$ and $R_{int,W}$ was marked in anesthetized, paralyzed healthy young men, and similar to that between $R_{vel,L}$ and $R_{vel,W}$, τvel being the same in both species (1.28±0.44 vs 1.20±0.18 s; p=0.399) (D'Angelo et al., 1991; 2000). Although for the conditions above energy dissipation would be greater for the lung also in supine men, in humans R_{ED} should increase with increasing f; indeed, using available parameters for unrestrained chest expansion from normal EELV (D'Angelo et al., 1991; 1994b; 2000), R_{ED} changes with f according to $R_{ED}=1.63+1.11 \cdot (1-e^{-2.9 \cdot f})$.

In all the species studied with the present approach, $R_{vel,L}$ was found to be markedly greater than $R_{vel,W}$, the ratio $R_{vel,L}/R_{vel,W}$ being about 1.5, 1.8, 2, and 2.6 in men (D'Angelo et al., 2000), dogs (Similowski et al., 1989 and present study), cats (Shardonofsky et al., 1991). and rabbits (D'Angelo et al., 2002; 2007; 2008), respectively. The main reason for this difference resides most likely in the contribution of surface phenomena to $R_{vel,L}$, because alterations of lung surfactant properties produced in normal rabbits by dioctylsodiumsulfosuccinate administration caused marked changes of $R_{vel,L}$ (D'Angelo et al., 2007). Interestingly, the analysis of the slow, post-occlusion pressure decay that followed inflations of various $\dot{V}$ and fixed V_T, has shown that lung lavage causes a marked increase in the pressure loss due to tissue viscoelasticity with no change in the time constant, but leaves the flow (viscous) related pressure changes unaffected (Perez Fontan,

1993). Bronchomotor tone can also contribute to $R_{vel,L}$; indeed, administration of histamine or methacholine increases lung tissue viscance in rabbits and dogs, besides airway flow resistance (Lutchen and Jackson, 1990; Romero and Ludwig, 1991; Tepper et al., 1992). Considering that changes in respiratory system mechanics induced by bronchoactive drugs reflect those of the lung, it is interesting to note that with increasing bronchoconstriction caused by histamine administration in anesthetized, paralyzed dogs (Bates et al., 1986), the changes of $R_{int,RS}$ and $R_{vel,RS}$ (R_1 and R_2 in that study) were significantly related ($r=0.705$; $p=0.01$). Consistent with this observation, when in the present dogs the lungs were widely exposed to the ambient, a significant increase of $R_{vel,L}$ occurred only in those animals in which $R_{int,L}$ also increased (Fig. 6). We do not have any documented explanation for this increase, but its seems possible that the invasive surgical intervention and the exposure of the lung to the ambient might have occasionally caused the release of bronchoactive mediators.

4.4. Concluding remarks

This study has shown that the dynamic behaviour of the respiratory system and of its components can be satisfactorily characterized in terms of the relatively simple Mount's model in a large variety of conditions. The model has the advantage of allowing the identification of the physiological counterparts of the estimated parameters, and this allows in turn the interpretation of the measures obtained with the rapid and maintained end-inflation occlusion method in terms of the corresponding mechanical characteristic both under physiological and pathophysiological conditions. This procedure has been in fact used to assess the mechanical properties of the respiratory system in patients with a variety of pulmonary diseases (Broseghini et al., 1988; Eissa et al., 1991; Guérin et al., 1993; Pesenti et al., 1993; D'Angelo et al., 1997), as well as the effects of the therapeutic interventions aimed to normalize one or another of that properties.

In the present dogs, the tissue elements accounting for lung and chest wall viscoelasticity behaved linearly, greatly simplifying the mechanical description and the interpretation of the measurements. The investigated volume range extended from 20 to 70% of the estimated vital capacity, and in healthy young subjects mechanically ventilated with a fixed V_T, lung and chest wall viscoelastic parameters were independent of volume over most of the inspiratory capacity (D'Angelo et al., 2000). On the other hand, departure from linear tissue viscoelasticity, mainly with increasing tidal volumes, has been occasionally observed in cats (Shardonofski et al., 1991), rabbits (D'Angelo et al., 2007), and humans (Eissa et al., 1991; D'Angelo et al., 2000), indicating that further studies in this direction are warranted.

The observation that viscoelastic and standard mechanical properties of rib cage and abdomen mechanical are nearly the same, implies that during passive expansion of the relaxed respiratory system, asynchronous motion of rib cage and abdomen is avoided over most of the physiological range of breathing frequency, and hence no additional work is requested because of chest wall distortion. On the other hand, asynchrony is often observed during spontaneous breathing in animals and humans, both under normal and, especially, pathological conditions. Although under this condition chest wall distortion is mainly due to the pattern of respiratory muscle activity, the knowledge of rib cage and abdomen mechanical properties remains essential for the assessment of the work of distortion and its partition between these components. In this connection, the use of the present approach in paralyzed subjects coupled with measurements of compartmental flows and volume changes should provide the relevant information.

Finally, values of $R_{vel,L}$ and $\tau_{vel,L}$ obtained before and after chest opening have shown that the contribution of heterogeneity parallel lung units to the value of these parameters is small, even in the presence of the more pronounced heterogeneity obtainable in normal dogs. It seems unlikely that heterogeneity of parallel lung units might contribute in a substantially greater amount in humans, because in the head-up posture the top-to-bottom difference in regional lung expansion inferred from local transpulmonary pressure measurements in dogs is similar to that directly assessed in healthy subjects (D'Angelo et al., 1970; Milic-Emili et al., 1968). In patients, however, a marked increase of $R_{vel,L}$ and $\Delta R_{,L}$ was found in a variety of diseases which are known to be associated with substantially increased heterogeneity of lung regional expansion and presumably mechanical properties (Broseghini et al., 1988; Eissa et al., 1991; Guérin et al., 1993; Pesenti et al., 1993; D'Angelo et al., 1997). Although entirely attributed to increased contribution of lung heterogeneities, the enhanced stress relaxation might have also reflected alterations of tissue viscoelasticity; in all these studies, the changes of lung viscoelastic parameters were in fact essentially the same as those of the chest wall, which, however, should not exhibit heterogeneity of regional viscoelastic properties, as indicated by the independence of $R_{vel,W}$ and $\tau_{vel,W}$ on posture, shape, and pattern of motion observed in dogs. On the other hand, while changes of lung viscoelastic properties in COPD and ARDS can be reasonably attributed to alteration of surfactant, degree of tissue hydration, smooth muscle activation, misalignment and degradation of interstitial elements, it is difficult to relate the changes of chest wall tissue viscoelasticity to the effects of these diseases. Further investigation on this intriguing issue seems therefore opportune.

Acknowledgements

This research was in part supported by Ministero dell'Istruzione, dell'Università e della Ricerca Scientifica (MIUR) of Italy, Rome.

References

Agostoni, E., Zocchi, L., Macklem, P.T., 1988. Transdiapgragmatic pressure and rib motion in area of apposition during paralysis. J. Appl. Physiol. 65, 1296-1300.

ATS/ERS Task Force, 2005. Standardisation of spirometry. Eur. Respir. J. 26, 319-338.

Bates, J.H.T., Decramer, M., Chartrand, D., Zin, W.A., Boddener, A., Milic-Emili, J., 1985. Volume-time profile during relaxed in normal dogs. J. Appl. Physiol. 59, 732-737.

Bates, J.H.T., Decramer, M., Zin, W.A., Harf, A., Milic-Emili, J., Chang, H.K., 1986. Respiratory resistance with histamine challenge by single-breath and forced oscillation methods. J. Appl. Physiol. 61, 873-880.

Bates, J.H.T., Bacconier, M., Milic-Emili, J., 1988a. Theoretical analysis of the interrupter technique for measuring respiratory mechanics. J. Appl. Physiol. 64, 2204-2214.

Bates, J.H.T., Ludwig, M.S., Sly, P.D., Brown, K., Martin, J.G., Fredberg, J.J., 1988b. Interrupter resistance elucidated by alveolar pressure measurement in open-chest normal dogs. J. Appl. Physiol. 65, 408-414.

Bates, J.H.T., Brown, K., Kochi, T., 1989a. Respiratory mechanics in the normal dog determined by expiratory flow interruption. J. Appl. Physiol. 67, 2276-2285.

Bates, J.H.T., Abe, T., Romero, P.V., Sato, J., 1989b. Measurement of alveolar pressure in closed-chest dogs during flow interruption. J. Appl. Physiol. 67, 488-49.

Baydur, A., Behrakis, P.K., Zin, W.A., Jaeger, M., Milic-Emili, J., 1983. A simple method for assessing the validity of esophageal balloon technique. Am. Rev. Respir. Dis. 126, 788-791.

Briscoe, W.A., Dubois, A.B., 1958. The relationship between airway resistance, airway conductance and lung volume in subjects of different age and body size. J. Clin. Invest. 37, 1279-1285.

Broseghini, C., Brandolese, R., Poggi, R., Polese, G., Manzin, E., Milic-Emili, J., Rossi, A., 1988. Respiratory mechanics during the first day of mechanical ventilation in patients with pulmonary edema and chronic airway obstruction. Am. Rev. Respir. Dis. 138, 355-361.

Chelucci, G.L., Brunet, F., Paccaly, D., Milic-Emili, J., Lockhart, A., 1991. A single compartment model cannot describe passive expiration in intubated paralyzed humans. Eur. Respir. J. 4, 458-464.

D'Angelo, E., Bonanni, M.V., Michelini, S., Agostoni, E., 1970. Topography of the pleural surface pressure in rabbits and dogs. Respir. Physiol. 8, 204-229.

D'Angelo, E., Michelini, S., Miserocchi, G., 1973. Local motion of the chest wall during passive and active expansion. Respir. Physiol. 19, 47-59.

D'Angelo, E., Sant'Ambrogio, G., 1974. Direct action of the contracting diaphragm on the rib cage in rabbits and dogs. J. Appl. Physiol. 36, 715-719.

D'Angelo, E., Calderini, E., Torri, G., Robatto, F.M., Bono, D., Milic-Emili, J., 1989. Respiratory mechanics in anesthetized paralyzed humans: effects of flow, volume and time. J. Appl. Physiol. 67, 2556-2564.

D'Angelo, E., Robatto, F.M., Calderini, E., Tavola, M., Bono, D., Torri, G., Milic-Emili, J., 1991. Pulmonary and chest wall mechanics in anesthetized paralyzed humans. J. Appl. Physiol. 70, 2602-2610.

D'Angelo, E., Prandi, E., Milic-Emili, J., 1993. Dependence of maximal flow-volume curves on time-course of preceding inspiration. J. Appl. Physiol. 75, 1155-1159.

D'Angelo, E., Prandi, E., Marazzini, L., Milic-Emili, J., 1994a. Dependence of maximal flow-volume curves on time course of preceding inspiration in patients with chronic obstructive pulmonary disease. Am. J. Resp. Crit. Care Med. 150, 1581-1586.

D'Angelo, E., Prandi, E., Tavola, M., Calderoni, E., Milic-Emili, J., 1994b. Chest wall interrupter resistance in anesthetized paralyzed humans. J. Appl. Physiol. 77: 883-887.

D'Angelo, E., Agostoni, E., 1995. Statics of the chest wall. In: The Thorax, part A, ed. C. Roussos, M. Dekker, New York, pp. 457-493.

D'Angelo, E., Rocca, E., Milic-Emili, J., 1999. A model analysis of the effects of different inspiratory flow patterns on inspiratory work during mechanical ventilation. Eur. Respir. Monograph 4, 279-295.

D'Angelo, E., Tavola, E., Milic-Emili, J., 2000. Volume and time dependence of respiratory system mechanics in normal anaesthetized paralysed humans. Eur. Respir. J. 16, 665-672.

D'Angelo, E., Pecchiari, M., Baraggia, P., Saetta, M., Balestro, E., Milic-Emili, J., 2002. Low-volume ventilation causes peripheral airway injury and increased airway resistance in normal rabbits. J. Appl. Physiol. 92, 949-956.

D'Angelo, E., Pecchiari, M., Gentile, G., 2007. Dependence of lung injury on surface tension during low-volume ventilation in normal open-chest rabbits. J. Appl. Physiol. 102, 174–182.

D'Angelo, E., Koutsoukou, A., Della Valle, P., Gentile, G., Pecchiari, M., 2008. Cytokine release, small airway injury, and parenchymal damage during mechanical ventilation in normal open-chest rats. J. Appl. Physiol. 104, 41-49.

Deschamps, C., Rodarte, J.R., Wilson, T.A., 1988. Coupling between rib cage and abdominal compartments of the relaxed chest wall. J. Appl. Physiol. 65, 2265-2269.

Eissa, N.T., Ranieri, M., Corbeil, C., Chasse, M., Robatto, F.M., Braidy, J., Milic-Emili, J., 1991. Analysis of behavior of the respiratory system in ARDS patients: effects of flow, volume, and time. J. Appl. Physiol. 70, 2719-2729.

Estenne, M., Yernault, J.C., De Troyer, A., 1985. Rib cage and diaphragm-abdominal compliance in humans: effect of age and posture. J. Appl. Physiol. 59, 1842-1848.

Guérin, C., Coussa, M.-L., Eissa, N.T., Corbeil, C., Chasse, M., Braidy, J., Matar, N., Milic-Emili, J., 1993. Lung and chest wall mechanics in mechanically ventilated COPD patients. J. Appl. Physiol. 74, 1570-1580.

Hantos, Z., Daroczy, B., Suki, B., Galgoczy, G., Csendes, T., 1986. Forced oscillatory impedance of the respiratory system at low frequency. J. Appl. Phisiol. 60, 123-132.

Hantos, Z., Daróczy, B., Csendes, T., Suki, B., Nagy, S., 1990. Modeling of low-frequency pulmonary impedance in dogs. J. Appl. Physiol. 68, 848-860.

Harf, A., Decramer, M., Zin, W.A., Harf, A., Milic-Emili, J., Chang, H.K., 1986. Respiratory resistance in dogs by single-breath and forced oscillation methods. J. Appl. Physiol. 59, 262-265.

Hildebrandt, J., 1969. Dynamic properties of air-filled excised cat lung determined by liquid plethysmograph. J. Appl. Physiol. 27, 246-250.

Hildebrandt, J., 1970. Pressure-volume data of cat lung interpreted by a plastoelastic, linear viscoelastic model. J. Appl. Physiol. 28, 365-372.

Hughes, R., May, A.J., Widdicombe, J.G., 1959. Stress relaxation in rabbits' lungs. J. Physiol. London 146, 85-97.

Ingram, R.H., Pedley, T.J., 1986. Pressure-flow relationships in the lungs. Handbook of Physiology. Section 3. The Respiratory System. Volume 3: Mechanics of Breathing. Bethesda, MD, American Physiological Society, pp. 277-293.

Jiang, J.X., Demedts, T.S., Decramer, M., 1988. Mechanical coupling of upper and lower canine rib cages and its functional significance. J. Appl. Physiol. 19, 990-994.

Lorino, A.M., Lorino, H., Harf, A., 1994. A synthesis of the Otis, Mead, and Mount mechanical respiratory models. Respir. Physiol. 97, 123-133.

Lutchen, K.R., Jackson, A.C., 1990. Effects of tidal volume and methacholine on low-frequency total respiratory impedance in dogs. J. Appl. Physiol. 68, 2128-2138.

Milic-Emili, J., Henderson, J.A.M., Dolovich, M.B., Trop, D., Kaneko, K., 1966. Regional distribution of inspired gas in the lung. J. Appl. Physiol. 21, 749-759.

Mount, E., 1955. The ventilation flow resistance and compliance of rats lungs. J. Physiol. London 127, 157-167.

Pérez Fontán, J.J., 1993. Effect of lung lavage on the stress relaxation of the respiratory system J. Appl. Physiol. 75, 1536-1544.

Pesenti, A., Pelosi, P., Rossi, A., Aprigliano, M., Brazzi, L., Fumagalli, R., 1993. Respiratory mechanics and bronchodilator responsiveness in patients with the adult respiratory distress syndrome. Crit. Care Med. 21, 78-83.

Romero, P.V., Ludwig, M.S., 1991. Maximal methacholine-induced bronchoconstriction in rabbit lung: interactions between airways and tissue? J. Appl. Physiol. 70, 1044-1050.

Shardonofski, F.R., Skaburskis, M., Sato, J., Zin, W.A., Milic-Emili, J., 1991. Effects of volume history and vagotomy on pulmonary and chest wall mechanics in cats. J. Appl. Physiol. 71, 498-508.

Sharp, J.T., Johnson, F.N., Goldberg, N.B., Van Lith, P., 1967. Hysteresis and stress adaptation in the human respiratory system. J. Appl. Physiol. 23, 487–497.

Similowski, T., Levy, P., Corbeil, C., Bates, J.H.T., Jonson, B., Milic-Emili, J., 1989. Viscoelastic behavior of lung and chest wall in dogs determined by flow interruption. J. Appl. Physiol. 67, 2219-2229.

Stamenovic, D., Glass, G.M., Barnas, G.M., Fredberg, J.J., 1990. Viscoplasticity of respiratory tissues. J. Appl. Physiol. 69, 973-988.

Tepper, R., Sato, J., Suki, B., Martin, J.G., Bates, J.H.T., 1992. Low-frequency pulmonary impedance in rabbits and its response to inhaled methacholine. J. Appl. Physiol. 73, 290-295.

Wilson, T.A., 1994. Time constants may be meaningless in exponentials fit to pressure relaxation data. (Letter to Editor) J. Appl. Physiol. 77, 1570-1571.

Table 1 Interrupter resistance (Rint), quasi-static elastance (Est), viscoelastic resistance (Rvel) and time constant (τvel) of the respiratory system (RS), chest wall (W), and lung (L) obtained under various experimental conditions in 9 anesthetized, paralyzed dogs.

	SNOR	SRCB	p*	SETL	p*	H-UPNOR	p*	p†
$Rint_{RS}$, $cmH_2O \cdot s \cdot l^{-1}$	2.0±0.6	4.0±1.0	<0.001	1.6±0.5	0.004	1.6±0.2	0.046	1.000
$Rint_{W}$, $cmH_2O \cdot s \cdot l^{-1}$	0.9±0.3	2.3±1.2	0.020	0.8±0.3	0.271	0.8±0.3	0.461	1.000
$Rint_{L}$, $cmH_2O \cdot s \cdot l^{-1}$	1.1±0.4	1.8±1.0	0.476	0.8±0.4	0.012	0.8±0.3	0.043	1.000
Est_{RS}, $cmH_2O \cdot l^{-1}$	35.7±6.0	51.8±7.3	<0.001	38.1±5.0	0.618	42.1±5.1	0.002	0.004
Est_{W}, $cmH_2O \cdot l^{-1}$	10.0±1.3	21.9±5.9	<0.001	9.8±2.2	1.000	14.8±3.8	0.024	0.006
Est_{L}, $cmH_2O \cdot l^{-1}$	25.7±6.3	29.9±7.0	0.005	28.4±5.9	0.421	27.3±6.3	1.000	1.000
$Rvel_{RS}$, $cmH_2O \cdot s \cdot l^{-1}$	13.5±4.1	19.5±4.4	0.001	13.7±4.1	1.000	13.3±4.1	1.000	1.000
$Rvel_{W}$, $cmH_2O \cdot s \cdot l^{-1}$	4.7±2.2	10.1±3.8	0.003	4.8±2.3	1.000	5.0±2.4	1.000	1.000
$Rvel_{L}$, $cmH_2O \cdot s \cdot l^{-1}$	8.9±2.7	9.9±3.0	0.738	8.9±2.7	1.000	8.4±2.7	1.000	1.000
τvel_{RS} s	1.17±0.09	1.18±0.15	1.000	1.24±0.15	1.000	1.23±0.12	1.000	1.000
τvel_{W}, s	1.18±0.22	1.18±0.24	1.000	1.22±0.27	1.000	1.25±0.29	1.000	1.000
τvel_{L}, s	1.20±0.13	1.18±0.11	1.000	1.19±0.18	1.000	1.20±0.14	1.000	1.000

Values are mean±SD. SNOR: supine normal; SRCB: supine with rib cage block; SETL: supine with expiratory threshold load; H-UPNOR: head-up normal.*compared to SNOR; † H-UPNOR compared to SETL.

Table 2 Interrupter resistance (Rint), quasi-static elastance (Est), viscoelastic resistance (Rvel) and time constant (τvel) of the lung (L) in 9 anesthetized, paralyzed head-up dogs before (H-UPNOR) and after wide opening of the thorax (H-UPOPN).

	H-UPNOR	H-UPOPN	p
$Rint_{,L,\ cmH_2O \cdot s \cdot l^{-1}}$	0.8±0.3	1.6±0.8	0.013
$Est_{,L,\ cmH_2O \cdot l^{-1}}$	27.3±6.3	27.7±7.3	0.844
$Rvel_{,L,\ cmH_2O \cdot s \cdot l^{-1}}$	8.4±2.7	9.4±2.9	0.054
$\tau vel_{,L,\ s}$	1.23±0.14	1.19±0.05	0.874

Values are mean±SD.

Table 3 Viscoelastic resistance (Rvel) and time constant (τvel) of the lung (L) in 4 anesthetized, paralyzed open-chest dogs before and after heart arrest.

	$R_{vel,L}$, $cmH_2O \cdot s \cdot l^{-1}$			$\tau_{vel,L}$, s		
	before	after		before	after	
dog	5 s*	5 s	20 s	5 s	5 s	20 s
1	9.5	9.5	9.5	1.40	1.41	1.41
2	8.2	8.3	9.2	1.22	1.17	1.19
3	15.5	14.4	14.6	1.18	1.21	1.20
4	7.3	8.1	8.2	1.18	1.10	1.07
mean±SD	10.2±3.7	10.1±2.9	10.4±2.9	1.24±0.10	1.22±0.13	1.22±0.14
p		0.857†	0.250#		0.448†	0.641#

*Time from the end-inspiratory occlusion at which the fall of transpulmonary pressure ($P_{2,L}$) was measured for Rvel and τvel assessment. †compared to data before heart arrest; #compared to data obtained at 5 s after heart arrest.

Legends

Fig. 1. The temporal sequence with which the experimental conditions were studied, together with the concomitant changes in airway opening pressure (Pao), end-expiratory lung volume (EELV), and end-expiratory esophageal pressure (Pes,e-e), and the indication of the performed interventions.

Fig. 2. Panel A: The relationships between inflation flow and lung or chest wall interrupter resistance (Rint). Panel B: The relationships between volume above the end-expiratory lung volume (EELV) in the supine posture at zero airway opening pressure and lung and chest wall Rint or lung conductance (Gint). Open symbols: supine dogs with unrestrained chest mechanically ventilated from normal EELV. Closed symbols: head-up dogs or supine animals with expiratory threshold load. Numbers are slope of the linear functions or describe the curvilinear relation. Here and in all the other figures, points are mean±SE of the average values obtained in a given condition in 9 anesthetized, paralyzed dogs.

Fig. 3. The relationships between the duration of inflation and the additional resistance (ΔR) of the respiratory system (RS), lung (L), and chest wall (W) in supine dogs with normal expansion of the chest (sNOR) or impeded expansion of the rib cage (sRCB). Points were fitted using *Eq.1*.

Fig. 4. The quasi-static inflation P-V curve of lung and chest wall in the supine (open symbols) and head-up posture (closed symbols). Dotted circles refer to the chest wall of supine dogs with impeded expansion of the rib cage.

Fig. 5. The relationships between the duration of inflation and the additional resistance (ΔR) of the respiratory system (RS), lung (L), and chest wall (W) in supine dogs ventilated from normal (sNOR) or elevated end-expiratory lung volume (sETL) and in head-up dogs (eNOR). In these conditions, test breaths of fixed V_T and various $\dot{V}$ were applied, whereas in supine dogs ventilated from normal EELV test breaths of fixed $\dot{V}$ and various V_T (sNOR-iso $\dot{V}$) were also applied. Points were fitted using *Eq.1*.

Fig. 6. The changes of lung viscoelastic resistance ($R_{vel,L}$) with wide chest wall opening in 4 and 5 dogs in which $R_{int,L}$ either did not (Group #1), or did change significantly (Group #2). Bars are SE.

Fig. 7. Electrical analogue of the respiratory system and its components.

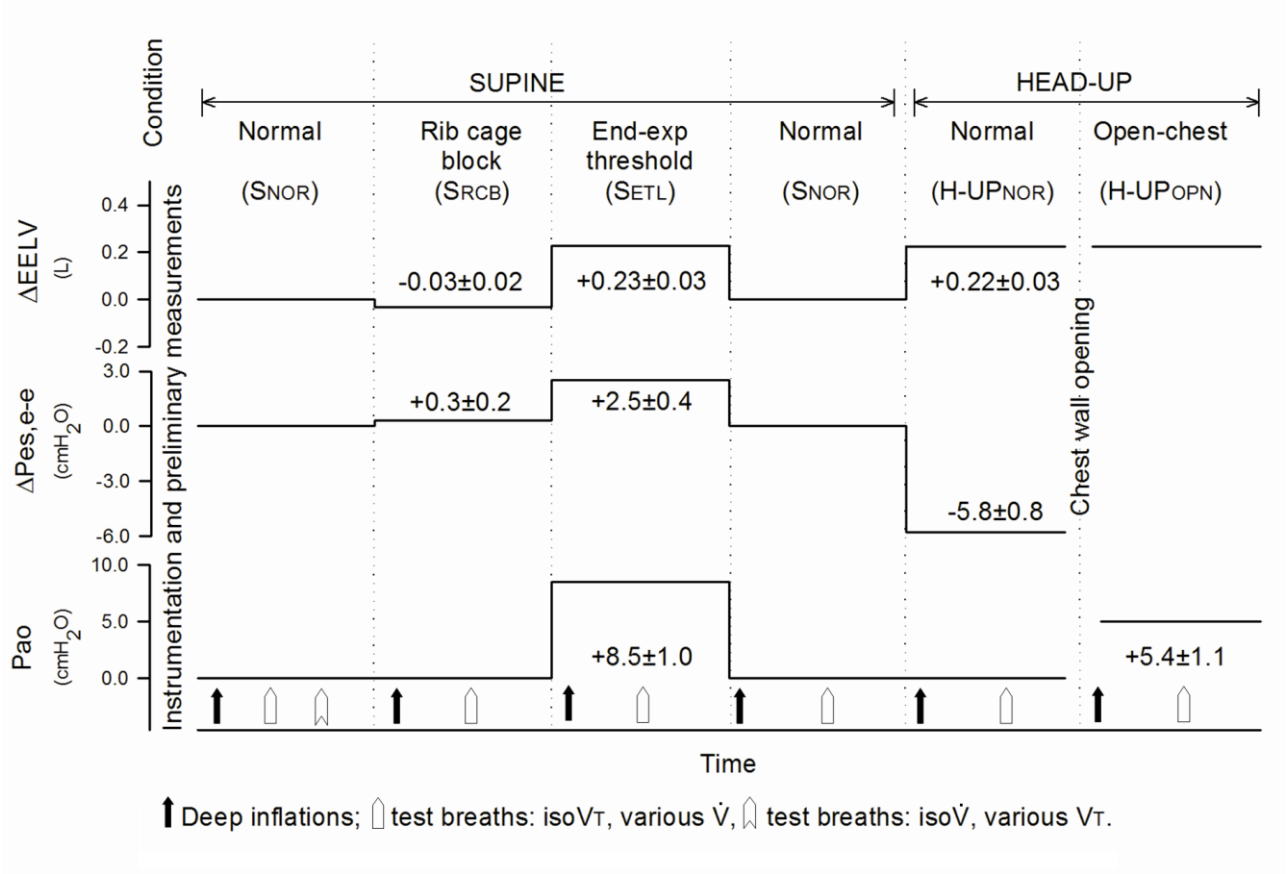
Condition
SUPINE
HEAD-UP
Normal
(SNOR)
Rib cage block
(SRCB)
End-exp threshold
(SETL)
Normal
(SNOR)
Normal
(H-UPNOR)
Open-chest
(H-UPOPN)
ΔEELV (L)
0.4
0.2
0.0
-0.2
-0.03±0.02
+0.23±0.03
+0.22±0.03
ΔPes,e-e (cmH2O)
3.0
0.0
-3.0
-6.0
+0.3±0.2
+2.5±0.4
-5.8±0.8
Pao (cmH2O)
10.0
5.0
0.0
+8.5±1.0
+5.4±1.1
Chest wall opening
Instrumentation and preliminary measurements
Time
Deep inflations; test breaths: isoVT, various V̇, test breaths: isoV̇, various VT.

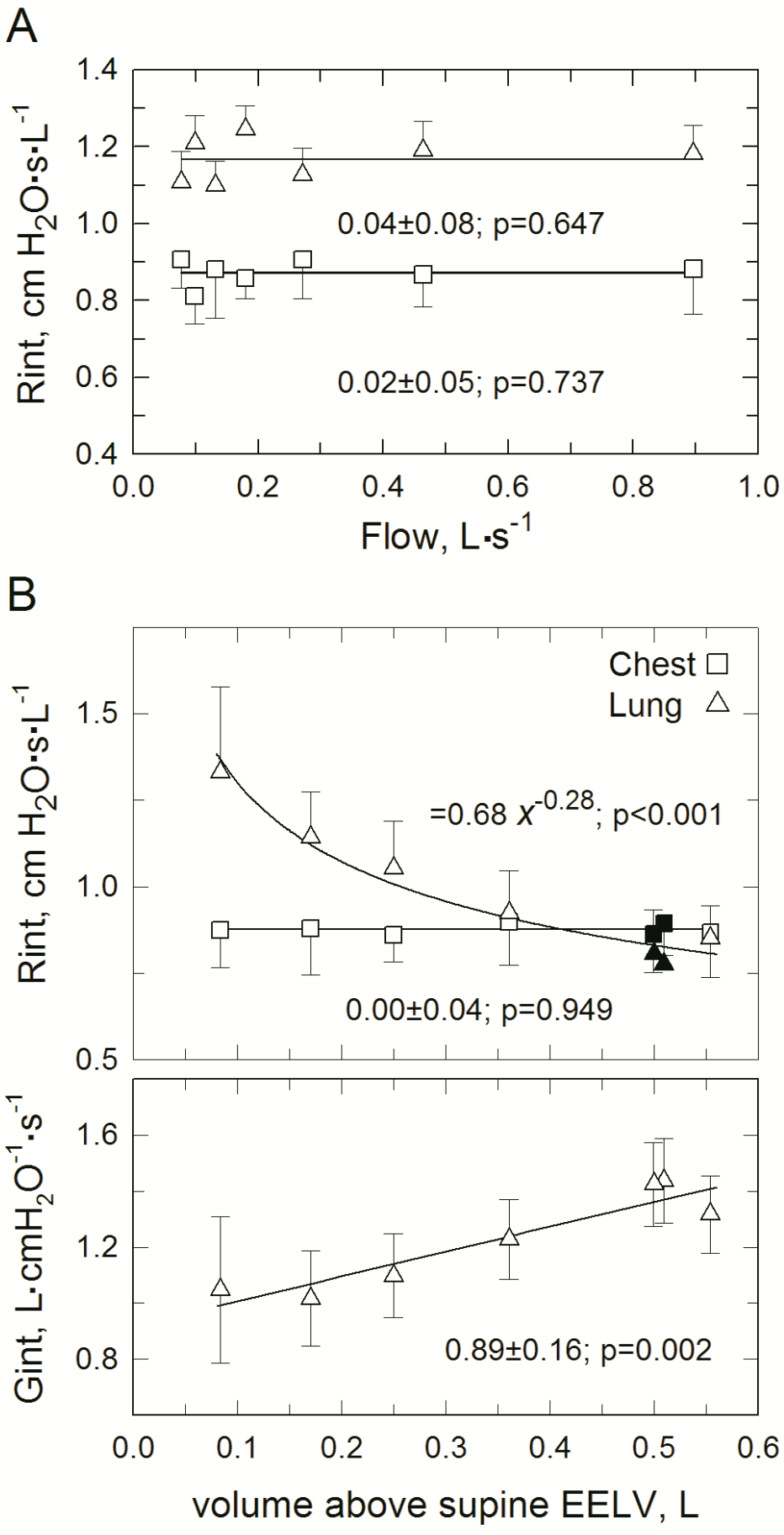
A
1.4
1.2
1.0
0.8
0.6
0.4
Rint, cm H2O·s·L-1
0.04±0.08; p=0.647
0.02±0.05; p=0.737
0.0
0.2
0.4
0.6
0.8
1.0
Flow, L·s-1
B
Chest
Lung
1.5
1.0
0.5
Rint, cm H2O·s·L-1
=0.68 x-0.28; p<0.001
0.00±0.04; p=0.949
1.6
1.2
0.8
Gint, L·cmH2O-1·s-1
0.89±0.16; p=0.002
0.0
0.1
0.2
0.3
0.4
0.5
0.6
volume above supine EELV, L

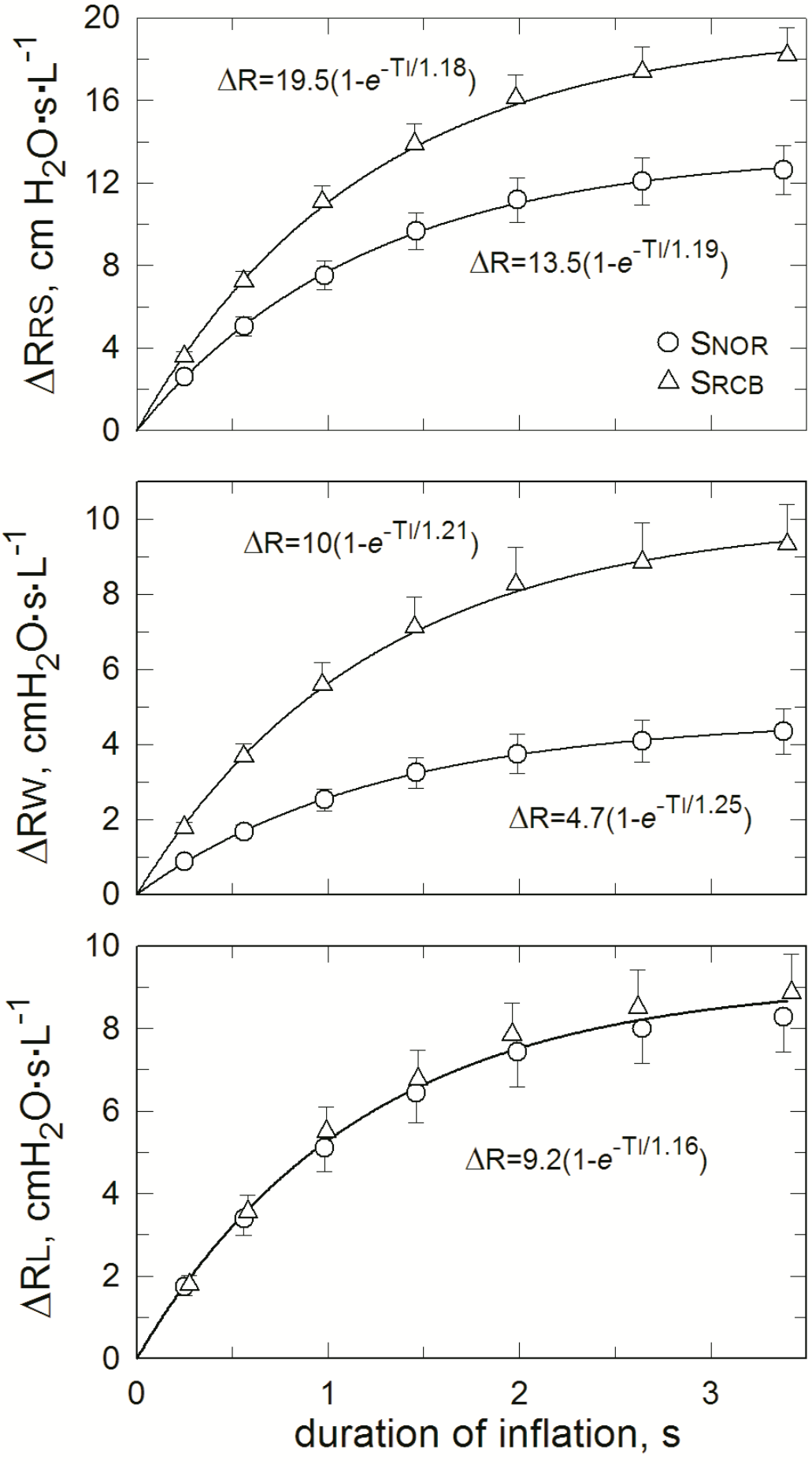
ΔRRS, cm H2O·s·L-1
ΔR=19.5(1-e-TI/1.18)
ΔR=13.5(1-e-TI/1.19)
SNOR
SRCB
ΔRW, cmH2O·s·L-1
ΔR=10(1-e-TI/1.21)
ΔR=4.7(1-e-TI/1.25)
ΔRL, cmH2O·s·L-1
ΔR=9.2(1-e-TI/1.16)
duration of inflation, s

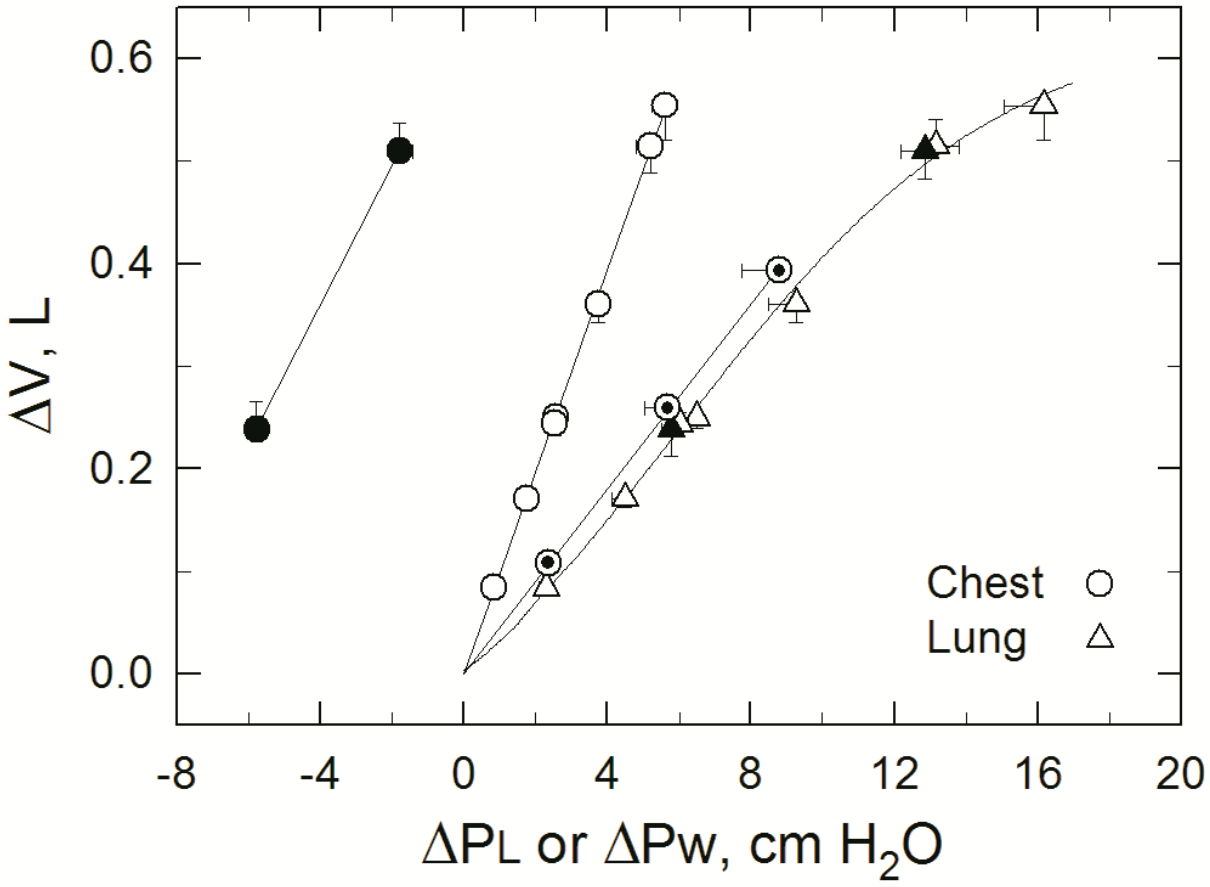
0.6
0.4
0.2
0.0
ΔV, L
-8
-4
0
4
8
12
16
20
ΔPL or ΔPw, cm H2O
Chest
Lung

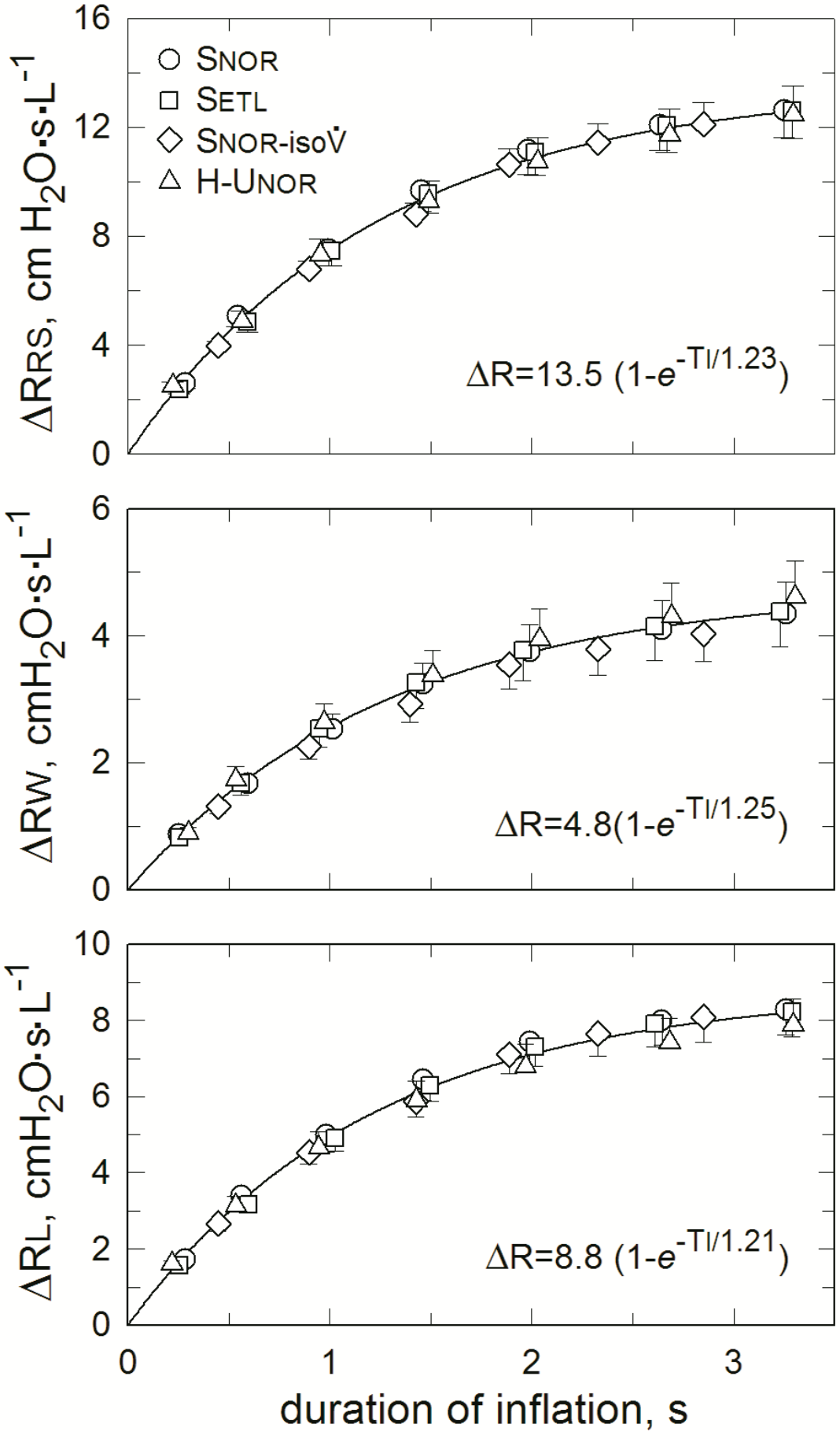
SNOR
SETL
SNOR-isoV
H-UNOR
ΔRRS, cm H2O·s·L-1
ΔR=13.5 (1-e-TI/1.23)
ΔRW, cmH2O·s·L-1
ΔR=4.8(1-e-TI/1.25)
ΔRL, cmH2O·s·L-1
ΔR=8.8 (1-e-TI/1.21)
duration of inflation, s

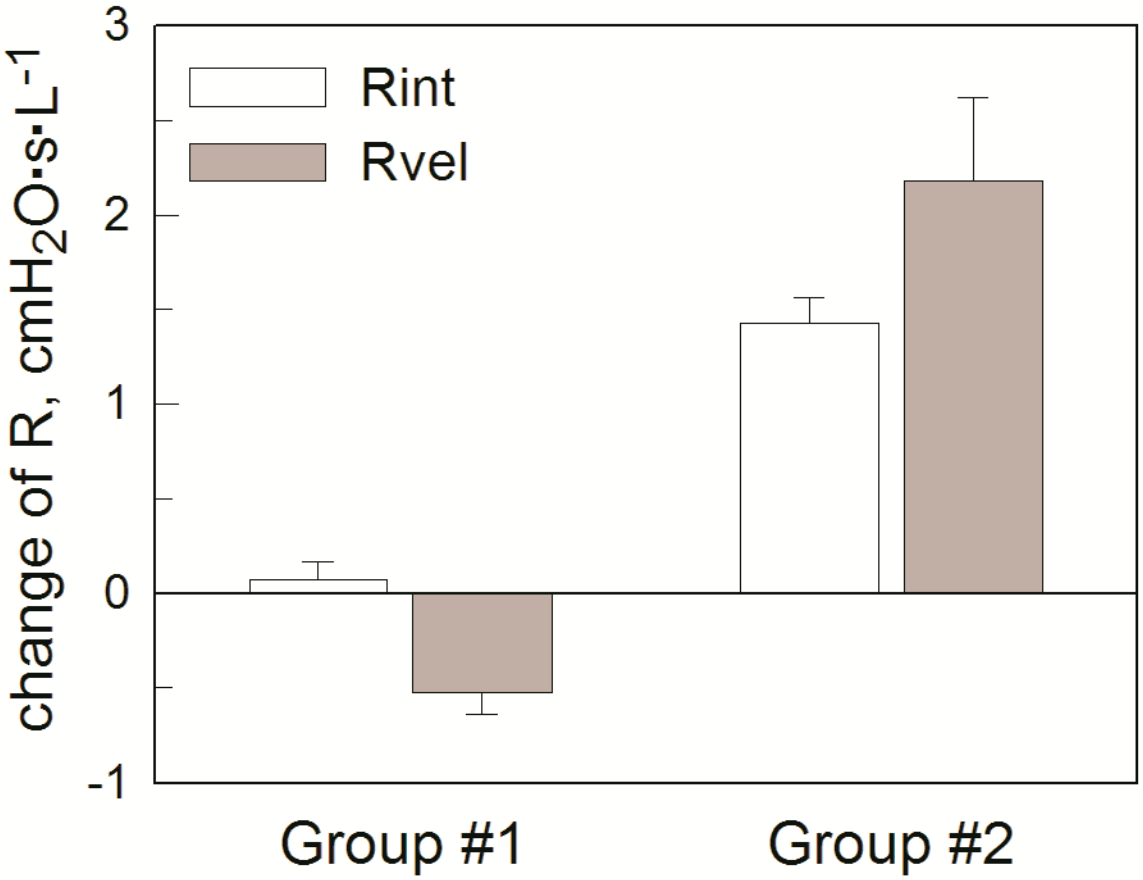
change of R, cmH2O·s·L-1
3
2
1
0
-1
Rint
Rvel
Group #1
Group #2

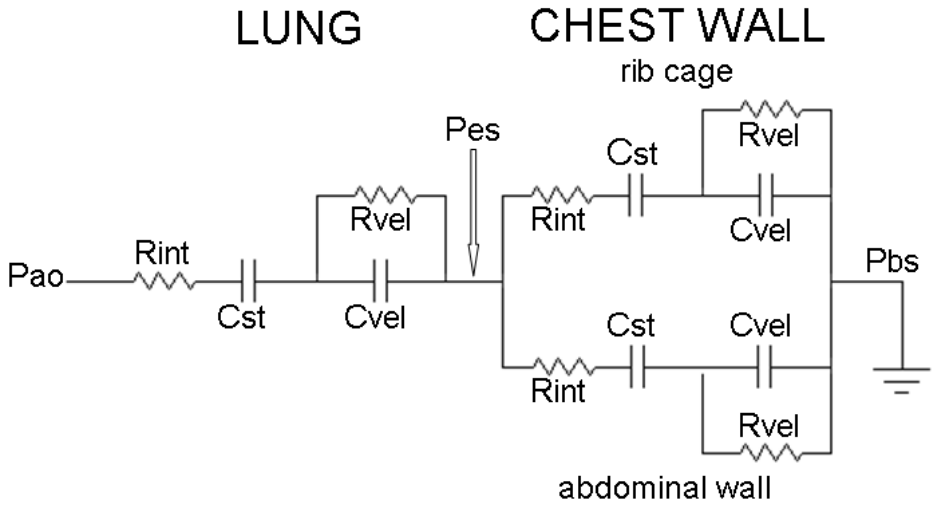
LUNG
CHEST WALL
rib cage
Pes
Rvel
Cst
Rvel
Rint
Cvel
Pao
Rint
Pbs
Cst
Cvel
Cst
Cvel
Rint
Rvel
abdominal wall